

Full Paper

Determination of Paraquat in Fruits and Natural Water using Ni(OH)₂ Nanoparticles-Carbon Nanotubes Composite Modified Carbon Ionic liquid Electrode

Reza Faramarzi,¹ Ali Reza Taheri,^{1,*} Mahmoud Roushani²

¹*Islamic Azad University – Ilam Branch, Ilam, Iran*

²*Department of Chemistry, Ilam University, Ilam, Iran*

* Corresponding Author, Tel.: +988432246039; Fax: +988432246045

E-Mail: Taheri@ilam-iau.ac.ir; Alirezachem@yahoo.com

Received: 26 April 2015 / Received in revised form: 16 October 2015 /

Accepted: 22 October 2015 / Published online: 31 December 2015

Abstract- A novel analytical approach has been developed and evaluated for the quantitative analysis of paraquat herbicides which can be found at trace levels in the presence of ascorbic acid and uric acid. The experimental results suggest that a carbon ionic liquid electrode modified with multi-walled carbon nanotubes and nickel hydroxide nanoparticles accelerates the electron transfer reactions of paraquat. The best responses were obtained with differential potential and chronoamperometry methods in Phosphate buffer (pH, 7.5). The influence of various parameters on the electrode was investigated. Under the optimized working conditions, calibration graphs were linear in the concentration ranges of 0.0025–25 mg L⁻¹ with a detection limit (S/N=3.0) of 0.8 ppb. The proposed electrode was used for determination of paraquat in fruits and River water samples with satisfactory results.

Keywords- Paraquat, Room temperature ionic liquid, Nickel hydroxide nanoparticles, Multiwalled carbon nanotubes, Carbon ionic liquid electrode

1. INTRODUCTION

Paraquat (1,1-dimethyl-4,4-bipyridinium dichloride) a fast-acting non-selective contact herbicide, is one of the most widely used herbicides owing to its high efficacy and low

environmental persistence. Paraquat (PQ) is used in weeding many crops and there have been many authenticated cases of detection of its residues in water sources [1]. Its residues constitute a potential danger for health since it is a highly persistent molecule when present in the environment. This fact increases the contamination risk when paraquat is overused. Therefore, there is an urgent need to determine paraquat in the environment, air and food. PQ is polar, highly soluble in water and has a low volatility.

However, since paraquat has significant acute toxicity and there is no specific antidote against paraquat [2,3], fatalities are often caused by accidental or voluntary ingestion of paraquat [4].

During the past few decades, paraquat (PQ) has proved to be a popular agent for intentional poisonings. Paraquat is extremely toxic to humans (LD50 35 mg/kg) and animals (rats: LD50 is 110–150 mg/kg), by all means of exposure. Since recently, the use of PQ has been restricted [5,6]. In order to offer sufficient medical treatment for paraquat poisoning, it is important to identify the ingested poison and estimate the dose amount. Several methods have been reported for the analysis of paraquat using Colorimetry [7], spectrophotometry [8], capillary electrophoresis [9], gas and liquid chromatography [10], post-column colorimetric detection [11] and mass spectrometry [12]. However these methods suffer from some disadvantages including long analysis times, high costs, the requirement for sample pretreatment, and in some cases low sensitivity and selectivity. These disadvantages probably make them unsuitable for routine analysis. The advantages of electrochemical methods for determination of paraquat include low cost, high sensitivity and short measurement time. Literature has so far reported different electroanalytical approaches in order to determine paraquat [13,14]. They are mainly based on the voltammetry technique [15,16]. An increase in the sensitivity of electroanalytical methods, using chemically modified electrodes, can be achieved by its combination with an effective method of pre-concentration. The basic carbon electrode materials most frequently used for electrochemical measurements are glassy carbon and carbon paste electrode [16].

The subtle electronic behavior of carbon nanotubes (CNTs) reveals that they have the ability to mediate electron transfer reactions of electroactive species in solution when used as an electrode modifier [17]. Additionally, transition-metal nanoparticles, in different forms, have emerged as a novel family of catalysts able to promote more efficiently a variety of organic transformations because of their small size and extremely large surface-to-volume ratio [18]. Recently several different types of nanoparticles have been successfully introduced onto CNTs, such as Au [19], Cu [20], Ag [21], Co [22,23] and Ni [24-26] in metallic, oxide and hydroxide form for fabrication of sensors.

Compared to the other materials, Ni with natural abundance is relatively low-cost, making it suitable for the fabrication of sensors in batch. In contrast to Ni nanomaterials which are unstable and easily oxidized in air and solution, the hydroxide and oxide of nickel(II) are

relatively stable [27,28]. Nickel hydroxide Nanoparticles (NiHNPs) with a small crystalline size shows a high proton diffusion coefficient, which leads to excellent electrochemical performance.

Many methods for preparing nickel hydroxide nanoparticles (NiHNPs) such as coordination precipitation, precipitation transformation, hydrothermal conversion, urea homogeneous precipitation, and micro emulsion, need harsh reaction conditions such as high temperature or pressure [29]. Some methods use organic solvents which increase the production cost [30]. However the method of coordination homogeneous precipitation (CHP) is new and facile, without needing expensive raw materials or equipment. It is also easy for mass production, and can be applied to the synthesis of various hydroxide or oxide nanocrystals [31,32].

Room temperature ionic liquids (RTILs) such as 1-butyl-3-methylimidazolium hexafluorophosphate, (BMIM)(PF₆), are compounds that composed of ions and exist in the liquid state below 298 K[33]. Because of their high stability, high electrical conductivity and very low vapor pressure, RTILs hold great promise for green chemistry applications in general and for electrochemical applications in particular[34]. Recently, preparation of electrodes modified with a composite of room-temperature ionic liquids and carbon nanotubes have gained increasing attention for combining their desirable benefits to develop the performances of electrochemical sensing [35,36]. This new composite has several advantages compared to using graphite and other traditional carbon paste and composite electrodes, where it offers improved sensitivities toward a number of compounds, and at the same time lower detection potentials using a very small amount of MWCNTs [36].

In the present work an RTIL, (BMIM)(PF₆), is used as the binder for fabrication of a carbon ionic liquid electrode (CILE) then modified with a nanocomposite film which contains MWCNTs and NiHNPs, based on the idea that the MWCNTs with NiHNPs could enhance the electron transfer rate for PQ, due to synergistic electrocatalysis which leads to increasing the sensitivity. The fabricated MWNTs-NiHNPs/CILE results in excellent sensitivity, wide linear range, favorable stability and reproducibility and a low detection limit. The analytical performance of the electrode has been evaluated in fruits and natural water samples with satisfactory results.

2. EXPERIMENTAL

Paraquat was purchased from Aldrich; the multiwalled carbon nanotubes (MWCNTs) of 20–30 nm in diameter and 0.5–2.0 μm in length; purity: ≥95% were purchased from Sigma. Spectrally pure graphite powder (average particle size 50 μm) from Merck was used as received. A stock solution of PQ (5 mg/L) was prepared by dissolving the required amount of the compound; all solutions were prepared with ultra-pure water. 0.1 mol L⁻¹ Phosphate buffer solution (PBS) was prepared by dissolving appropriate amounts of sodium hydrogen

phosphate and sodium dihydrogen phosphate in a 250 mL volumetric flask. The pH of the buffer was adjusted to appropriate value by addition of 7.5 mol L⁻¹ sodium hydroxide solution. All electrochemical experiments were carried out in 0.1 mol L⁻¹ PBS at pH 7.5. Other reagents were of analytical grade purchased from Merck and used without further purification.

2.1. Synthesis of Nanoscale Ni(OH)₂

Nanoscale Ni(OH)₂ was synthesized using a simple coordination precipitation procedure as previously reported [31]. Briefly, by adding concentrated ammonia (28 wt.%) to nickel (II) nitrate solution (1 M), a deep blue colored nickel hexammine complex solution was formed and added into a given amount of distilled water, the reaction was carried out under magnetic stirring for 1 h at 70 °C. Finally, light green sediments were formed. The precipitate was separated by centrifuge and rinsed with distilled water and ethanol three times respectively to remove the adsorbed ions, then dried in a vacuum oven at 80 °C for 12 h. The final product was a green powder. Product that is obtained without any surfactant in the reaction process was platelet-like shape.

2.2. Electrode modification

The carbon ionic liquid electrode (CILE) was prepared by mixing graphite powder and BMIMPF₆ (w/w 4:1) thoroughly in a mortar to form a carbon paste. A portion of the carbon paste was firmly filled into one end of a glass tube (ca. 1.8 mm i.d. and 10 cm long) and a copper wire was inserted through the opposite end to establish an electrical contact. The surface of the CILE was smoothed on a piece of weighing paper. The fabricated CILE was used as the basic solid electrode. A stock solution of MWCNTs–NiHNPs in DMF was prepared by dispersing weighed amounts of MWCNTs and NiHNPs (94%:5% w/w) in 1 mL DMF using ultrasonic bath until a homogeneous solution resulted, and 20 µL of the prepared suspension was pipetted onto the CILE surface with a microsyringe and dried at room temperature. a small bottle was fitted tightly over the electrode so that the solvent could evaporate slowly and a uniform film was formed. The fabricated electrode was stored at 4 °C when not in use. For comparison, CILE, MWCNTs/CILE, NiHNPs/CILE and NiHNPs-MWCNTs/CILE, were prepared with similar procedures and used for further investigation.

2.3. Instrumentation

All the voltammetric measurements were carried out using our Ni(OH)₂ nanoparticles-carbon nanotubes composite modified carbon Ionic liquid electrode, (NiHNPs/MWCNT/CILE) as the working electrode, Ag/AgCl, 3 mol L⁻¹ KCl as the reference electrode

and platinum wire as an auxiliary electrode. Electrochemical measurements were performed using a μ AUTOLAB TYPE III. The pH measurements were performed with a Metrohm 744 pH meter using a combination glass electrode. X-ray diffraction (XRD) measurements were performed at a speed of $0.01^\circ \text{ s}^{-1}$ by a Bruker Axs diffractometer (Germany) with Cu $K\alpha$ ($\lambda=1.5418 \text{ nm}$) operating at 40 kV, 30 mA. The morphology of the nanoscale NiHNPs was investigated by scanning electron microscopy (SEM, Leica Cambridge, model S 360) and transmission electron microscopy (TEM, Philips CM10).

2.4. General procedure

Each sample solution (30 mL) containing 0.1 mol L^{-1} phosphate buffer solution (pH 7.5) and an appropriate amount of PQ was pipetted into a voltammetric cell. Unless stated otherwise, all voltammetry measurements were preceded by 45 s accumulation time at open circuit potential in analyte solution.

The voltammograms were recorded by applying positive-going potential from -1.5 to 0.0 V. After every measurement, the electrode was regenerated by soaking then rinsing thoroughly with triply distilled water and then 0.5% sodium hydroxide solution for few seconds to remove adsorbed substances. The electrode was finally rinsed carefully with distilled water to remove all adsorbate from the electrode surface and to provide a fresh surface before running the next experiments. All sample solutions were deoxygenated by purging with N_2 gas before each experiment.

3. RESULTS AND DISCUSSION

3.1. Characterization of $\text{Ni}(\text{OH})_2$ nanoparticles

Nanoscale $\text{Ni}(\text{OH})_2$ was characterized by means of SEM and TEM. Fig. 1a shows a typical image of the nanoscale $\text{Ni}(\text{OH})_2$ synthesized via coordination precipitation method and MWNTs.

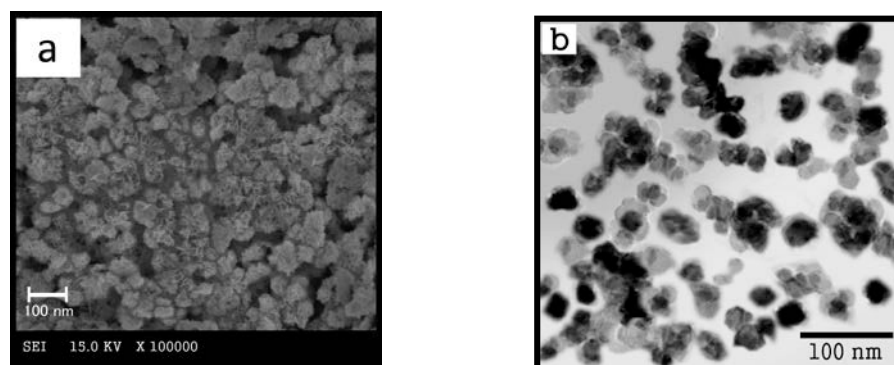


Fig. 1. SEM image of the MWNTs and NiHNPs on glassy carbon (a) and TEM image of nickel hydroxide powders (b)

It can be observed that it appears to have a platelet-like shape and with a dimension of 50–80 nm, and weak agglomeration can be seen. Fig. 1b displays TEM image of nanoscale Ni(OH)₂. The result shows the nanoparticles are in the same sizes as it is shown in the SEM image.

The XRD pattern of the nanoscale Ni(OH)₂ is exhibited in Fig. 2. It can be seen that several diffraction peaks appear at $2\theta=19^\circ$, 34° , 39° , 52° , 58° , 62° , 71° and 74° , which can be indexed to planes (0 0 1), (1 0 0), (1 0 2), (1 1 0), (1 0 2), (1 1 1), (1 0 3) and (2 0 1) of β -Ni(OH)₂ according to JCPDS card no. 14-0117, respectively. Previous reports have indicated that peaks (0 0 1) and (1 0 1) were especially broad when the nickel hydroxide was more active [37,38]. Delmas and Tessier also considered a correlation between the electrochemical activity and the XRD pattern of nickel hydroxide. Also, another work from Delmas and coworkers determined this type of pattern to be associated with very poorly crystallized nickel hydroxide, denoted as β bc (bc: badly crystallized)[39]. This material, obtained by the ageing of β -nickel hydroxide, has very broad (0 0 1) and (1 0 1) lines in its XRD pattern, with narrow (hk0) lines. However the XRD pattern of this sample is very similar to the β bc-nickel hydroxide. A broadening of the (1 0 1) line for nanoscale Ni(OH)₂ can be seen, which is ascribed to the disordered structure of the material. Thus, the broadening of the (0 0 1) reflection is caused by the smaller crystalline size, as previously reported [40].

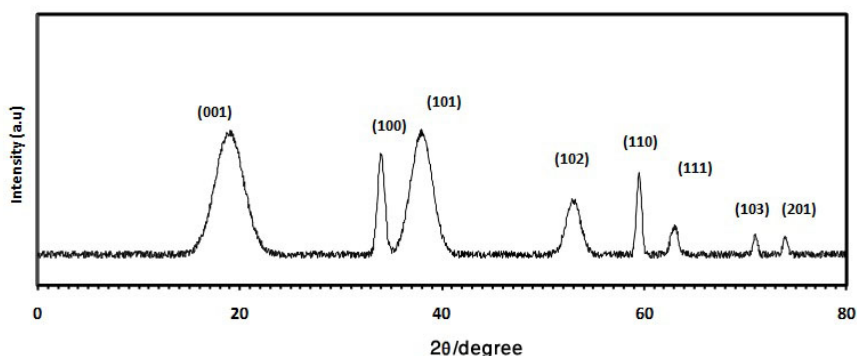
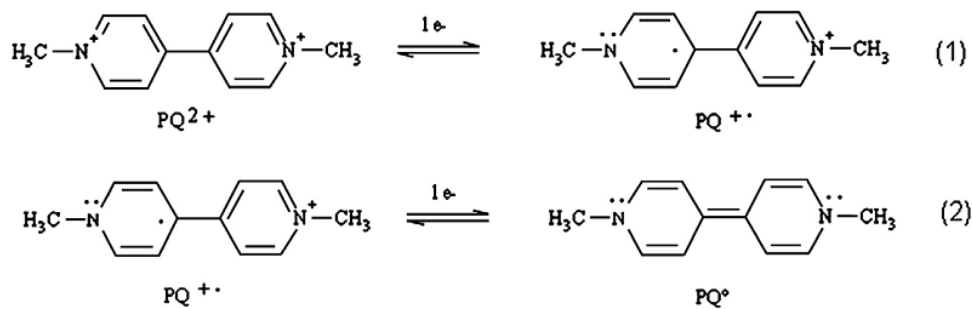


Fig. 2. Typical X-ray diffraction patterns of NiHNPs

3.2. Electrochemical behavior of paraquat

As shown in Scheme 1, the electroreduction of PQ²⁺ proceeds in two steps related to the reduction of the two positively charged quaternary nitrogen atoms of paraquat dication (PQ²⁺). The first monoelectronic reduction step, the blue radical cation (PQ^{•+}) is yield and the further reduction involving one electron, neutral PQ⁰ compound is obtained. These illustrations are consistent with those described elsewhere for paraquat [41].



Scheme 1. Suggested mechanism of electrochemical reduction of paraquat

Although, as a precautionary measure, all solutions were de-aerated by bubbling pure nitrogen gas prior to each electrochemical measurement, we did not observe any detectable effect on the analytical response of the electrodes when solutions were not de-aerated, indicating that residual oxygen in the sample solutions has no observable effect on the adsorption of paraquat.

The electrochemical behavior of paraquat at the different composite films in pH 7.5 phosphate buffer was investigated using cyclic voltammetry (CV) Fig. 3 shows the cyclic voltammograms of CILE, MWCNTs/CILE, NiHNPs/CILE, MWCNTs-NiHNPs/CILE. It can be seen (curves A in Fig. 3) that a broad oxidation peak and ill-defined redox waves appeared at the CILE electrode and the peak potentials of paraquat was indistinguishable while using the MWCNTs/CILE electrode two reductions peaks were observed towards the negative sweep direction, the first one around -0.63 V and the second at approximately -0.98 V versus SCE.

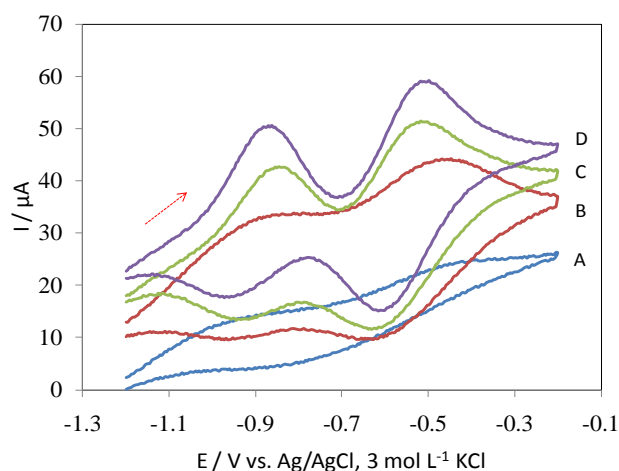


Fig. 3. CVs recorded of 2.5 mg L^{-1} paraquat at CILE (A), MWCNTs/CILE (B), NiHNPs/CILE (C), and MWCNTs-NiHNPs/CILE (D). Scan rate: 100 mV S^{-1}

These results could be explained the presence of MWCNTs can be increase the sensitivity. This is due to the fact that the electron transfer at carbon nanotubes electrodes could be better facilitated by the edge-plane-like nanotube ends. It can also be seen that the peak currents of paraquat increases further at the NiHNPs modified CILE as a result of the nano-size effect of NiHNPs (curves C in Fig. 3). The enhancement in peak currents and the lowering of over potentials are clear evidences of the catalytic effects of NiHNPs toward paraquat redox reaction. Curves D in Fig. 3 strongly suggests that the hybrid film of MWNTs and NiHNPs can combine the advantages of all of them and accelerate electron transfer significantly; therefore, result in remarkably increased response towards the redox of paraquat in contrast to MWNTs or NiHNPs alone. The mechanism can be described in Scheme 1. These illustrations are consistent with those described elsewhere for paraquat [42].

3.3. Optimization of Experimental Variables

Modification of a CILE with different amounts MWCNTs and NiHNPs was tested ($n=5$). The amount of NiHNPs influences the sensitivity of the sensor. It was found that as the composition of NiHNPs increased from 2 to 5%, the response of the electrode improved and when the composition was more than 5%, the response decreased with a larger background current, which resulted in poor measurements for paraquat (Fig. 4). So, 20 μL of 5% nanoscale NiHNPs (95% MWNTs) were chosen for the fabrication of the sensor. The oxidation peak currents of paraquat after 45 s accumulation at different potentials from 0.50 V to 0.10 V remained almost stable, revealing that potential does not affect the oxidation peak currents of paraquat. In contrast to potential, accumulation time strongly influences the peak currents.

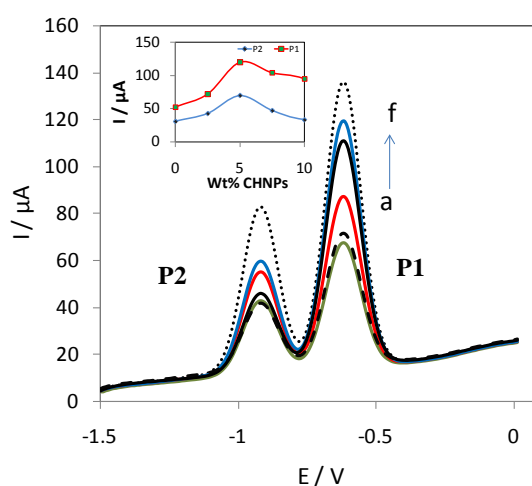


Fig. 4. Effect of the ratio of NiHNPs nanoscale on the sensor response ($n=5$), Insets: plot of peak current vs. ratio of NiHNPs percent. Pulse Amplitude: 50 mV; pulse width: 50 ms; scan rate=5 mV S^{-1} , accumulation time: 45 s

Fig. 5 shows the variations of differential pulse anodic peak currents of paraquat with respect to accumulation times. The anodic peak currents improve with accumulation time, but after 45 s remained almost stable. This may be due to saturation of the amount of paraquat adsorbed on the modified electrode surface. Thus, the accumulation time of 45 s was selected as an optimum time for subsequent experiments.

Subsequently, the effect of the supporting electrolyte upon the electrochemical sensing of paraquat was next explored; Britton-Robinson, ammonium, acetate and phosphate buffer solutions at pH value of 7.5 (all solutions in 0.1 mol L^{-1}) were investigated. The optimum result in terms of highest analytical signal was obtained using a 0.10 mol L^{-1} phosphate buffer solution, which was consequently selected for further studies Fig. S1 (Electronic Supplementary electronic supplementary Information; ESI). In the literatures, phosphate supporting electrolytes have been widely used for the analysis of organic compounds because of low background currents and good stability deposited [43-48].

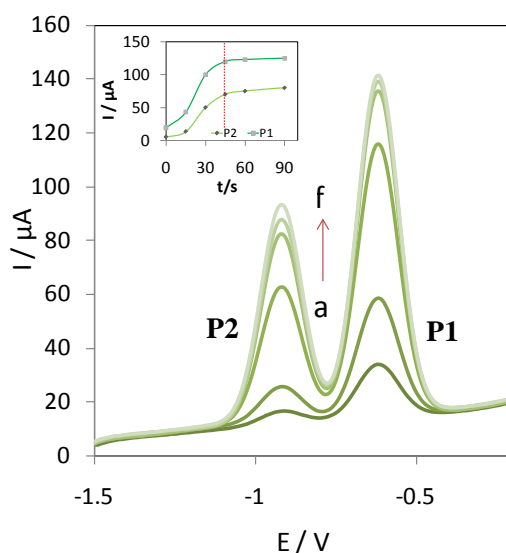


Fig. 5. The variations of differential pulse anodic peak currents of 2.5 mg L^{-1} paraquat with respect to accumulation time. Inset: plot of peak current vs. time

3.4. Effect of pH

The effect of the buffer pH on the electrochemical response was investigated by recording the differential pulse voltammograms of 2.5 mg L^{-1} paraquat in phosphate buffer solutions over the pH range from 4.5 to 9.5. As can be seen in Fig 6, the peaks currents, i_{P1} and i_{P2} gradually increase with the increase of pH and reached a maximum value when the pH is 7.5. The peak potentials do not, however, seem to be affected by the concentration of H^+ , suggesting the absence of any protonation step in the reduction mechanism reported in Scheme 1 [49], which is in close agreement with published works [16]. Therefore, pH 7.5 was chosen for subsequent measurements.

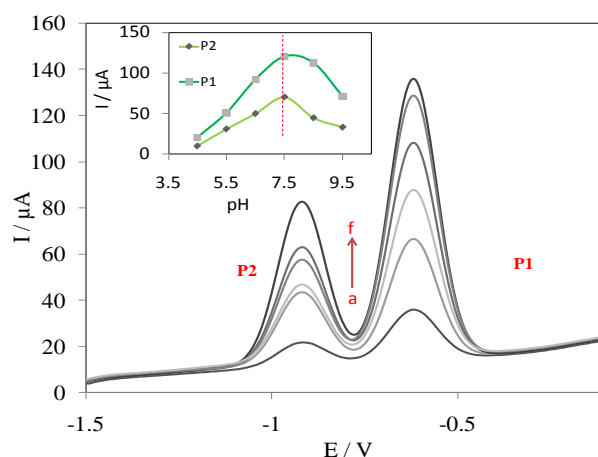


Fig. 6. DPVs of MwCNTs-NiHNPs/CILE in 0.1 mol L⁻¹ PBs at different pHs from 4 to 8 in 2.5 mg L⁻¹ paraquat, Insets: plot of peak current vs. pH values, Scan rate: 100 mV s⁻¹

3.5. Effect of the scan rate

In order to investigate the kinetics of electrode reactions, the cyclic voltammetric response arising from the electrochemical reduction of paraquat at different scan rates (in the range of 0.01 to 0.4 V s⁻¹) was explored with the dependence of peak current (PQ⁺²) upon the scan rate presented (Fig. 7).

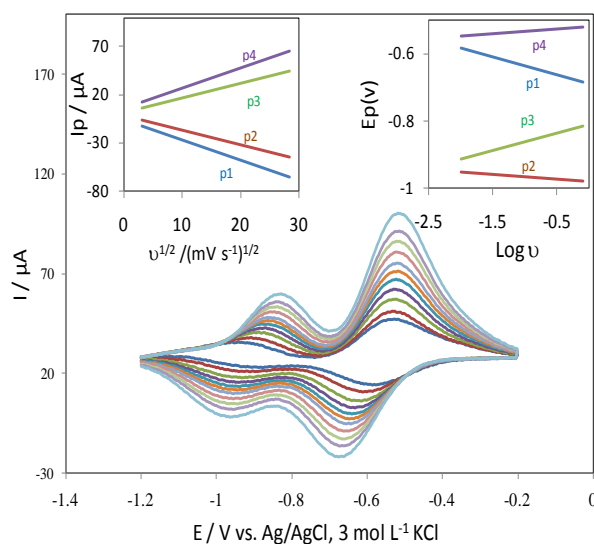


Fig. 7. Cyclic voltammograms of paraquat at different scan rates (from A to L) 10, 25, 75, 100, 125, 150, 200, 250, 300, 350 and 400 mV S⁻¹. Left Inset: dependence of peak currents vs. scan rate, Right Inset: dependence potentials vs. Log v

As can be observed, a linear relationship between peak current and the square root of the scan rate is readily obtained (insets of Fig. 7), which confirms an diffusion-controlled process on the surface of electrode in the studied range of potential sweep rates, with following equations:

$$I_{p1} = -2.11 v^{1/2} - 5.55 \quad (R^2 = 0.998) \quad (1)$$

$$I_{p_{a,1}} = -1.55 v^{1/2} - 1.18 \quad (R^2 = 0.998) \quad (2)$$

The E_{pa} shifted to more positive values with increasing the scan rate (v) suggesting the electron transfer is quasi-reversible.

3.6. Voltammetric responses of paraquat

The electrochemical response of additions of paraquat from 0.0005 to 50.00 mg L⁻¹ under the optimized conditions by DPV techniques using MWCNTs-NiHNPs/CILE is depicted in Fig. 8a. From Fig. 8b, the detection (DL) and quantification limits (QL) were obtained for the experimental conditions employed the criterions presented in Section 2.

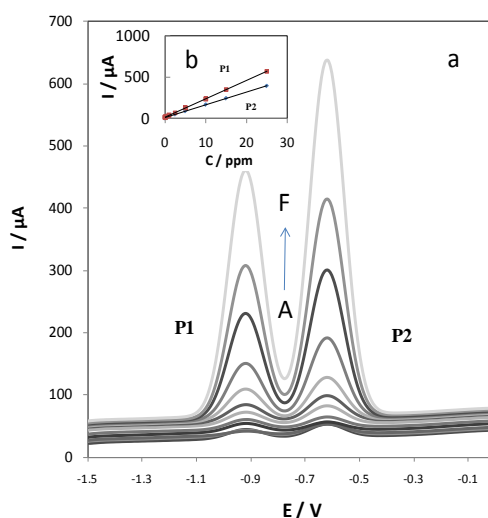


Fig. 8. DPVs of Paraquat at MWCNTs- NiHNPs /CILE in pH 7.0 PBS. Paraquat concentration (from A to F): 0.0025, 0.0050, 0.0100, 0.0500, 0.1000, 0.5000, 1.000, 2.500, 5.000, 10.000, 15.000, 25.000 mg L⁻¹ (a); Insets: the calibration curves of related species (b)

Table 1 shows the experimental results obtained, where the equations for analytical curve, the correlation coefficient (r), which determines the degree of linearity of the relationship between the concentration of pesticide and peak current, the standard deviation of the arithmetic mean of 10 blank solutions (S_b), the slope of the working curve (s), the detection limit (DL) the quantification limit (QL), and the analytic sensitivity of the DPV for peaks 1

and 2. Such results are shown to be very appropriate for the determination of ultra-traces of paraquat in natural water, where the recommended maximum residue stipulated by the European Community [50] is 10 ppb.

Table 1. Results obtained from linear regression curves (Fig. 8) for the determination of paraquat in pure electrolyte on MwCNTs-NiHNPs/CILE using DPV

Parameter	Peak 1	Peak 2
Equation	$I_p(\mu\text{A}) = 15.521C(\text{mg L}^{-1}) + 5.212$	$I_p(\mu\text{A}) = 21.871C(\text{mg L}^{-1}) + 10.228$
LDR/ mg L^{-1}	0.0025-25	0.0025-25
SD/ μA	0.001	0.0008
DL/ mg L^{-1}	0.0006	0.0004

Fig. 9 displays a chronoamperogram of the response of a rotated modified electrode (2500 rpm) following the successive injection of Paraquat at applied potential of 0.75 V in PBS (pH 7.5). For Paraquat the linear dynamic range was from 0.01 to 28.306 mg L^{-1} , with a calibration equation of $I_p(\mu\text{A}) = 1.3C(\text{mg L}^{-1}) + 3.15$ ($R^2 = 0.9977$) (Fig. 9B). A detection limit of 0.006 mg L^{-1} ($S/N=3$) was obtained.

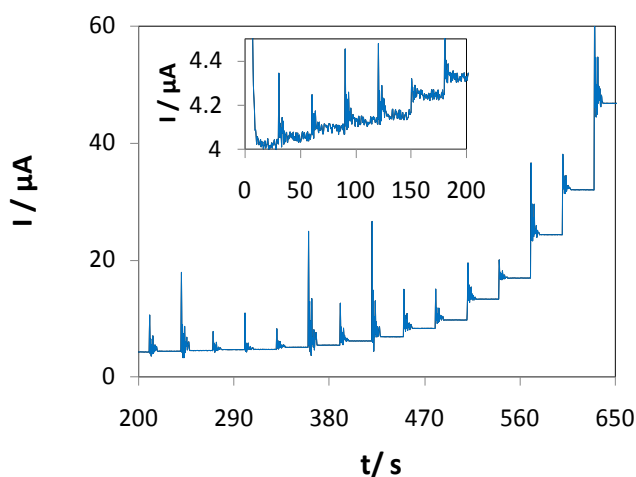


Fig. 9. Hydrodynamic amperometric response (rotating speed 2500 rpm) held at 0.75 V in PBS (pH 7.5) by successive additions of paraquat. Inset; plot magnification from 0 to 200 S

3.7. Repeatability and stability of the paraquat Sensor

To evaluate the repeatability of the MWCNTs- NiHNPs/CILE, the peak currents of 20 successive measurements by DPV in 2.5 mg L^{-1} paraquat was determined. The relative standard deviation (R.S.D.) of 1.14% and 0.47% was obtained for peak 1 and 2, respectively,

indicating that the MWCNTs-NiHNPs/CILE is not subject to surface fouling by the oxidation products.

The stability of the proposed sensor was investigated. After 60 cyclic runs, the voltammetric response to 2.5 mg L⁻¹ Paraquat almost remained 82.11% and 87.56% of the initial response, respectively (data not shown). The storage stability of the proposed biosensor was also studied. When not in use, the electrode was suspended above PBS at 4 °C in a refrigerator. After 7 days at 4 °C, the sensor retained 90.42% and 92.80% of its initial response current for peak 1 and 2, respectively. Indicating the film has a long lifetime.

3.8. Effects of interferences on the behavior of paraquat

In order to evaluate the selectivity of the proposed method, some common interferences were tested under optimized conditions. It was observed that anions such as NO₃⁻, CO₃²⁻, PO₄³⁻, Cl⁻, SO₄²⁻ and humic acid in a standard solution containing 2.5 mg L⁻¹ of paraquat did not change the profile of DP voltammograms obtained at any concentration. The Cd²⁺ cation supplied a small peak at -0.80 V of DP voltammograms which caused a slight interference of 1.1% in the baseline when added in 100:1 ratio. The Mg²⁺, Ca²⁺, Fe³⁺, Hg²⁺, Ni²⁺, cations did not significantly change the peak in 150:1 ratio. The tolerance limit was defined as the concentrations of foreign substances, which gave an error less than ±5.0% in the detection of the analyte. Upon addition of 2.5 mg L⁻¹ of paraquat, sensitive oxidation peaks appear and even 200 and 300 times AA and UA respectively had nearly no interference for the determination of PQ, suggesting that the Ionic liquid/ NiHNPs nanoparticles-carbon nanotubes composite modified CILE responds selectively to PQ. It shows that the proposed method is free from interferences of the most common interfering agents.

3.9. Application to fruits and River water samples

Paraquat is one of the most widely used herbicides in citric fruit cultures. Due to its toxicity and persistence in the environment, there is a very high probability of its contaminating crops, thus presenting a risk to human health. The juices were extracted from their respective fruits without any pre-separation or pre-concentration and had their pH values adjusted to 7.50 with NaOH solution. An aliquot of the 10 mL of each sample was added to the electrochemical cell for the posterior recovery experiments. The methodology was hence applied to orange, lemon and apple juices. No paraquat was detected in these samples so they were spiked with appropriate amounts of paraquat. Recovery curves for the samples spiked with 1 mg L⁻¹ paraquat. Based on the repeated differential pulse voltammetric responses (n=3) of the diluted analyte and the samples that were spiked with specified concentration of PQ, measurements were made for determination of PQ concentrations in food samples. The results are listed in Table 2. The results presented in Table 2 employing the proposed method

and the comparative GC/MS method¹⁰ are in good agreement at a confidence level of 96% (F test and paired t-test) and in agreement with the EPA [51] and Heath Canadian agency [52].

Table 2. Results obtained from recovery curves of paraquat in fruits samples considering peak 1 and peak 2

Sample		Detected value after spike/ mg L ⁻¹	Detected value after spike/ mg L ⁻¹	Rec. (%)
Orange	p1	0.95	0.95±0.003	95.1
	p2	0.96	0.96±0.002	96.2
Apple	p1	0.84	0.84±0.006	84.1
	p2	0.86	0.86±0.004	86.5
Lemon	p1	0.91	0.91±0.005	91.1
	p2	0.93	0.93±0.004	93.5

* Average of ten determinations at optimum conditions

The suitability of the proposed methodology for the analysis of paraquat in complex samples was checked by determining a small concentration of paraquat pesticide in natural water samples artificially spiked. The analytical procedure earlier described in the preceding sections was applied for natural water samples collected in 3 points in Seymareh River (Ilam-Iran), (for more information see Fig. S₂).

Table 3. Results obtained from recovery curves of paraquat in natural water samples considering peak 1 and peak 2

sample		Detected value after spike /mg L ⁻¹	Rec. (%)	comparative method (GC/MS) [10]
electrolyte	p1	2.48 ±0.02	99.2	2.45 ±0.02
	p2	2.49 ± 0.01	99.6	2.49 ± 0.01
Poin 1	p1	2.52 ±0.03	100.8	2.53 ±0.03
	p2	2.48 ±0.02	99.2	2.47 ±0.02
Poin 2	p1	2.46 ±0.03	98.4	2.41 ±0.03
	p2	2.41 ±0.03	96.4	2.43 ±0.03
Poin 3	p1	2.42 ±0.04	96.8	2.47 ±0.04
	p2	2.51 ±0.03	100.4	2.49 ±0.03

* Average of ten determinations at optimum conditions

As mentioned before, the sampling points were selected based on the different levels of organic matter, including industrial and domestic pollution in the sampling points. Recovery curves for the samples spiked with 2.5 mg L⁻¹ paraquat. The results of the present study are shown in Table 3, for peaks 1 and 2. In all samples, the percentage recovered obtained for peak 1 and peak 2 presented satisfactory values for the proposed electroanalytical methods [51] thus indicating the suitability of the proposed method for use in natural water samples.

The electrochemical parameters for determination of paraquat were compared with the earlier reports and the results were listed in Table 4. It can be seen that the present method combines high sensitivity, wide linear range and comparable detection limits.

Table 4. Comparison of the proposed electrode in paraquat determination with other types of nanocomposite material modified electrode

Electrode	Method	LDR/ $\mu\text{mol L}^{-1}$	DL/ $\mu\text{mol L}^{-1}$	References
HDME	SWV	0.05-10	0.015	[14]
PGE	SWV	0.5-29	0.1	[54]
CPE	SWV	0.8-20	0.015	[55]
Au microelectrode	SWV	4.3-140	0.039	[56]
BIFE	DPV	6.6-48	0.093	[57]
MWCNTs-NiHNPs /CILE	DPV	p1: 0.004-291.6 (0.001 -75 ppm)	0.0002	This work
		P2: 0.004-291.6 (0.001 -75 ppm)	0.0003	
	Chronoamperometry	0.038-110.048	0.0023	

4. CONCLUSIONS

Trace determination of paraquat was achieved by using MWCNTs-NiHNPs/CILE. The modified CILE was fabricated by a casting method, and the resulting electrode exhibited a good electrocatalytic performance to paraquat because of the combining of NiHNPs and MWCNTs. The electrode was used for determination of paraquat in real biological samples and satisfying results were achieved. The simple fabrication procedure, wide linear range, low detection limit, high stability and good reproducibility for repeated determination suggest that this electrode will be a good and attractive candidate for practical applications.

Acknowledgments

The authors gratefully acknowledge the research council of Islamic Azad University – Ilam Branch for providing financial support for this work.

REFERENCES

- [1] L. Ritter, K. Solomon, P. Sibley, K. Hall, P. Keen, G. Mattu, and B. Linton, *J. Toxicol. Environ. Health Part A* 65 (2002) 142.
- [2] D. R. J. Oliveira, J. A. Duarte, A. S. Navarro, F. Remião, M. L. Bastos, and F. Carvalho, *Crit. Rev. Toxicol.* 38 (2008) 13.
- [3] Z. E. Suntres, *Toxicology* 180 (2002) 65.
- [4] K. Kudo, T. Ishida, W. Hikiji, Y. Usumoto, T. Umehara, K. Nagamatsu, A. Tsuji, and N. Ikeda, *Forensic Toxicol.* 28 (2010) 25.
- [5] M. M. Djukic, D. M. Jovanovic, M. Ninkovic, I. Stevanovic, K. Ilic, M. Curcic, and J. Vekic, *Chem. Biol. Interact.* 199 (2012) 74.
- [6] Y. H. Jo, K. Kim, J. E. Rhee, G. J. Suh, W. Y. Kwon, S. H. Na, and H. B. Alam, *Resuscitation* 82 (2011) 487.
- [7] M. Gopal, C. D. Cohn, M. R. McEntire, and J. B. Alperin, *Am. J. Med. Sci.* 338 (2009) 373.
- [8] D. R. Jarvie, A. F. Fell, and M. J. Stewart, *Clin. Chim. Acta* 117 (1981) 153.
- [9] N. Mai, X. Liu, W. Wei, S. Luo, and W. Liu, *Microchim. Acta* 174 (2011) 89.
- [10] N. C. Posecion, E. M. Ostrea, and D. M. J. Bielawski, *Chromatogr. B* 862 (2008) 93.
- [11] S. Hara, N. Sasaki, D. Takase, S. Shiotsuka, K. Ogata, K. Futagami, and K. Tamura, *Anal. Sci.* 23 (2007) 523.
- [12] V. Y. Taguchi, S. W. D. Jenkins, P. W. Crozier, and T. D. Wang, *J. Am. Soc. Mass. Spectrom.* 9 (1998) 830.
- [13] D. D. Souza, and S. A. S. Machado, *Quim. Nova.* 26 (2003) 644.
- [14] A. Walcarius, and L. Lamberts, *J. Electroanal. Chem.* 406 (1996) 59.
- [15] E. Alvarez, M. T. Sevilla, J. M. Pinilla, and L. Hernandez, *Anal. Chim. Acta* 260 (1992) 19.
- [16] X. Ye, Y. Gu, and C. Wang, *Sens. Actuators B* 173 (2012) 530.
- [17] G. Che, B. B. Lakshmi, E. R. Fisher, and C. R. Martin, *Nature* 393 (1998) 346.
- [18] M. M. Manas, and R. Pleixats, *Acc. Chem. Res.* 36 (2003) 638.
- [19] T. J. Zhang, W. Wang, D. Y. Zhang, X. X. Zhang, Y. R. Ma, Y. L. Zhou, and L. M. Qi, *Adv. Funct. Mater.* 20 (2010) 1152.
- [20] X. Kang, Z. Mai, X. Zou, P. Cai, and J. Mo, *Anal. Biochem.* 363 (2007) 143.
- [21] C. Y. Liu, and J. M. Hu, *Biosens. Bioelectron.* 24 (2009) 2149.
- [22] A. Babaei, A. R. Taheri, and I. Khani, *Sens. Actuators B* 183 (2013) 265.

- [23] A. Babaei, A. R. Taheri, and M. Aminikhah, *Electrochim. Acta* 90 (2013) 317.
- [24] A. Babaei, and A. R. Taheri, *Sens. Actuators B* 176 (2013) 543.
- [25] A. Babaei, and A. R. Taheri, *Anal. Bioanal. Electrochem.* 4 (2012) 342.
- [26] A. Babaei, A. R. Taheri, and M. Sohrabi, *J. Electroanal. Chem.* 698 (2013) 45.
- [27] G. R. Fu, Z. A. Hu, L. J. Xie, X. Q. Jin, Y. L. Xie, Y. X. Wang, Z. Y. Zhang, Y. Y. Yang, and H. Y. Wu, *J. Electrochem. Sci.* 4 (2009) 1052.
- [28] A. Safavi, N. Maleki, and E. Farjami, *Biosens. Bioelectron.* 24 (2009) 1655.
- [29] M. Jayalakshmi, N. Venugopal, B. R. Reddy, and M. M. Rao, *J. Power Sourc.* 150 (2005) 272.
- [30] X. Liu, and L. Yu, *J. Power Sourc.* 128 (2004) 326.
- [31] G. X. Yan, and D. Cheng, *J. Mater. Lett.* 61 (2007) 621.
- [32] X. L. Li, J. F. Liu, and Y. D. Li, *Mater. Chem. Phys.* 80 (2003) 222.
- [33] M. J. Earle, and K. R. Seddon, *Pure Appl. Chem.* 72 (2000) 1391.
- [34] J. G. Huddleston, A. E. Visser, W. M. Reichert, H. D. Willauer, G. A. Broker, and R. D. Rogers, *Green Chem.* 3 (2001) 156.
- [35] C. Xiang, Y. Zou, L. X. Sun, and F. Xu, *Electrochem. Commun.* 10 (2008) 38.
- [36] Q. Wang, H. Tang, Q. Xie, L. Tan, Y. Zhang, B. Li, and S. Yao, *Electrochim. Acta* 52 (2007) 6630.
- [37] K. Watanabe, T. Kikuoka, and N. Kumagai, *J. Appl. Electrochem.* 25 (1995) 219.
- [38] C. Delmas, and C. Tessier, *J. Mater. Chem.* 7 (1997) 1439.
- [39] C. Faure, C. Delmas, and M. Fouassier, *J. Power Sourc.* 35 (1991) 279.
- [40] U. Köhler, C. Antonius, and P. Bäuerlein, *J. Power Sourc.* 127 (2004) 45.
- [41] D. D. Souza, and S. A. S. Machado, *Anal. Chim. Acta* 546 (2005) 85.
- [42] T. H. Lu, and I. W. Sun, *Talanta* 53 (2000) 443.
- [43] E. Shams, A. Babaei, A. R. Taheri, and M. Kooshki, *J. Biochem.* 75 (2009) 83.
- [44] A. Babaei, A. R. Taheri, and M. Afrasiabi, *J. Braz. Chem. Soc.* 8 (2011) 1549.
- [45] A. R. Taheri, A. R. Mohadesi, D. Afzali, H. Karimi, H. Mahmoudi, H. Zamani, and Z. Rezaeyati, *J. Electrochem. Sci.* 6 (2011) 171.
- [46] M. Afrasiabi, Z. Rezaeyati, S. H. Kianpour, A. Babaei, and A. R. Taheri, *J. Chem. Soc. Pak.* 4 (2013) 1106.
- [47] A. Babaei, M. Zendejdel, B. Khalilzadeh, and A. R. Taheri, *Coll. Surf. B* 66 (2008) 226.
- [48] A. Babaei, M. Afrasiabi, S. Mirzakhani, and A. R. Taheri, *J. Braz. Chem. Soc.* 22 (2011) 344.
- [49] R. M. Eloffson, and R. L. Edsberg, *Can. J. Chem.* 35 (1957) 646.
- [50] [online] available at: <http://europa.eu.int/comm/food/index.en.htm>
- [51] [online] EPA, available at:
<http://www.epa.gov/fedrgstr/EPA-PEST/2006/September/Day-06/p14642>.

- [52] [online] available at: Health Canadian Agency, <http://www.hc-sc.gc.ca/ewh-semt/altformats/hecssesc/pdf/pubs/water-eau/paraquat/paraquat-eng.pdf>
- [53] Analytical Methods Committee, Royal Society of Chemistry, Recommendations for the Definition, Estimation and Use of the Detection Limit Analyst. 112 (1987) 199.
- [54] I. C. Lopes, D. D. Souza, S. A. S. Machado, and A. A. Tanaka, *Anal. Bioanal. Chem.* 388 (2007) 1907.
- [55] L. C. S. Figueiredo-Filho, V. B. Dos Santos, B. C. Janegitz, T. B. Guerreiro, O. Fatibello-Filho, R. C. Faria, and L. H. Marcolino-Junior, *Electroanalysis* 2 (2010) 1260.
- [56] D. D. Souza, L. Codognoto, S. A. S. Machado, and L. A. Avaca, *Anal. Lett.* 38 (2005) 331.
- [57] M. A. El Mhammedi, M. Bakasse, and A. Chtaini, *J. Hazard. Mater.* 145 (2007) 1.